Vol. 10 (2017) *Acta Physica Polonica B Proceedings Supplement* No 4

MAGNETIZED QCD PHASE DIAGRAM*

Márcio Ferreira, Pedro Costa, Constança Providência

CFisUC, Department of Physics, University of Coimbra, Coimbra, Portugal

(Received August 21, 2017)

Using the (2+1)-flavor Nambu–Jona-Lasinio (NJL) model with the Polyakov loop, we determine the structure of the QCD phase diagram in an external magnetic field. Beyond the usual NJL model with constant couplings, we also consider a variant with a magnetic field-dependent scalar coupling, which reproduces the Inverse Magnetic Catalysis (IMC) at zero chemical potential. We conclude that the IMC affects the location of the Critical End Point, and found indications that, for high enough magnetic fields, the chiral phase transition at zero chemical potential might change from an analytic to a first-order phase transition.

DOI:10.5506/APhysPolBSupp.10.1197

1. Introduction

The properties of hadronic matter in a magnetized environment is attracting the attention of the physics community. The effect of an external magnetic field on the chiral and deconfinement transitions is an active field of research with possible relevance in multiple physical systems. From heavy-ion collisions at very high energies to the early stages of the Universe and astrophysical objects like magnetized neutron stars, the magnetic field may play an important role.

The catalyzing effect of an external magnetic field on dynamical chiral symmetry breaking, known as Magnetic Catalysis (MC) effect, is well-understood [1]. However, Lattice QCD (LQCD) studies show an additional effect [2–4], the Inverse Magnetic Catalysis (IMC): instead of catalyzing, the magnetic field weakens the dynamical chiral symmetry breaking in the crossover transition region. The chiral pseudo-critical transition temperature turns out to be a decreasing function of the magnetic field strength.

Different theoretical approaches have been applied in studying the magnetized QCD phase diagram, and specifically the IMC effect. Several low-energy effective models, including the Nambu–Jona-Lasinio (NJL)-type models, have been used to investigate the impact of external magnetic fields on quark matter (for a recent review, see [5]).

* Presented at "Excited QCD 2017", Sintra, Lisbon, Portugal, May 7–13, 2017.

2. Model

We perform our calculations in the framework of the Polyakov–Nambu–Jona-Lasinio (PNJL) model. The Lagrangian in the presence of an external magnetic field is given by

$$\begin{aligned}\mathcal{L} \;=\; & \bar{q}\left[i\gamma_\mu D^\mu - \hat{m}_f\right] q + G_s \sum_{a=0}^{8}\left[(\bar{q}\lambda_a q)^2 + (\bar{q}i\gamma_5\lambda_a q)^2\right] - \tfrac{1}{4}F_{\mu\nu}F^{\mu\nu} \\ & -K\left\{\det\left[\bar{q}\left(1+\gamma_5\right)q\right] + \det\left[\bar{q}\left(1-\gamma_5\right)q\right]\right\} + \mathcal{U}\left(\Phi,\bar{\Phi};T\right)\,,\end{aligned}$$

where $q = (u,d,s)^T$ represents a quark field with three flavors, $\hat{m}_f = \mathrm{diag}_f(m_u, m_d, m_s)$ is the corresponding (current) mass matrix, and $F_{\mu\nu} = \partial_\mu A_\nu^{\mathrm{EM}} - \partial_\nu A_\mu^{\mathrm{EM}}$ is the (electro)magnetic tensor. The covariant derivative $D^\mu = \partial^\mu - iq_f A^\mu_{\mathrm{EM}} - iA^\mu$ couples the quarks to both the magnetic field B, via A^μ_{EM}, and to the effective gluon field, via $A^\mu(x) = g\mathcal{A}_a^\mu(x)\frac{\lambda_a}{2}$, where $\mathcal{A}_a^\mu$ is the $\mathrm{SU_c}(3)$ gauge field. The q_f represents the quark electric charge ($q_d = q_s = -q_u/2 = -e/3$). We consider a static and constant magnetic field in the z direction, $A_\mu^{\mathrm{EM}} = \delta_{\mu 2}x_1 B$. We employ the logarithmic effective potential $\mathcal{U}\left(\Phi,\bar{\Phi};T\right)$ [6] fitted to reproduce lattice calculations.

We use a sharp cutoff (Λ) in three-momentum space as a model regularization procedure. The parameters of the model are [7]: $\Lambda = 602.3$ MeV, $m_u = m_d = 5.5$ MeV, $m_s = 140.7$ MeV, $G_s^0\Lambda^2 = 1.835$ and $K\Lambda^5 = 12.36$.

We analyze two model variants with distinct scalar interaction coupling: a constant coupling $G_s = G_s^0$ and a magnetic field-dependent coupling $G_s = G_s(eB)$ [8]. In the latter, the magnetic field dependence is determined phenomenologically by reproducing the decrease ratio of the chiral pseudo-critical temperature obtained in LQCD calculations [2]. Its functional dependence is $G_s(\zeta) = G_s^0\left(\frac{1+a\,\zeta^2+b\,\zeta^3}{1+c\,\zeta^2+d\,\zeta^4}\right)$, where $\zeta = eB/\Lambda_{\mathrm{QCD}}^2$ (with $\Lambda_{\mathrm{QCD}} = 300$ MeV). The parameters are $a = 0.0108805$, $b = -1.0133\times10^{-4}$, $c = 0.02228$, and $d = 1.84558\times10^{-4}$ [8].

3. Results (zero chemical potential)

Let us first compare both models at zero chemical potential. The up-quark condensate (all quarks show similar results), normalized by its vacuum value, and the Polyakov loop value are presented in Fig. 1. The presence of the IMC effect in the $G_s(eB)$ model is clearly seen in Fig. 1 (top, right panel), by the suppression effect of the magnetic field on the quark condensate around the transition temperature region. Furthermore, the $G_s(eB)$ model still leads to Magnetic Catalysis at low and high temperatures: the magnetic field enhances the quark condensate away from the transition temperature region, *i.e.*, at low and high temperatures. The chiral pseudo-critical transition temperature, defined as the inflection point of the quark condensate,

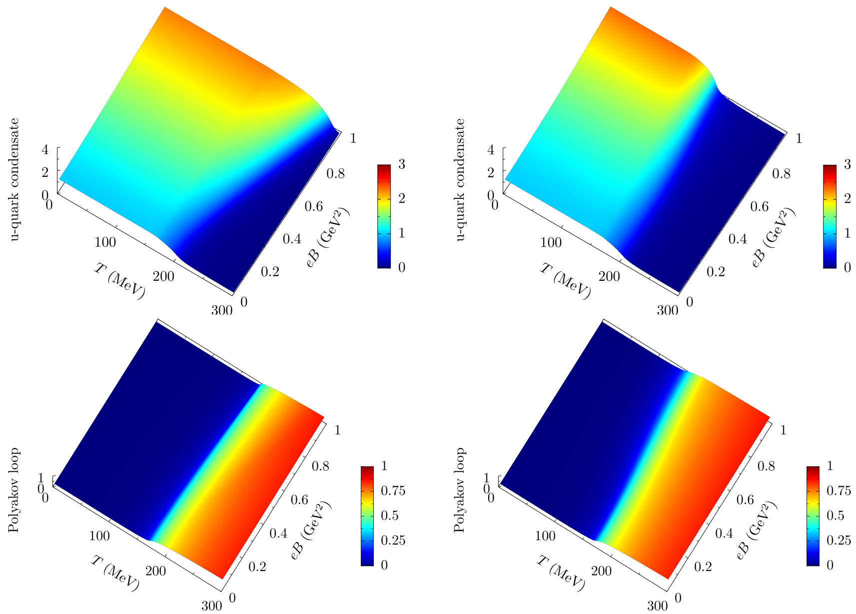

Fig. 1. Vacuum normalized u-quark condensate (top) and Polyakov loop value (bottom) for G_s^0 (left) and $G_s(eB)$ (right).

decreases for $G_s(eB)$ and increases for G_s^0. The $G_s(eB)$ makes possible not only the decreasing transition temperature, but also preserves the analytic nature of the chiral transition, in accordance with LQCD results. The $G_s(eB)$ dependence also affects the Polyakov loop value (bottom panel). A decreasing pseudo-critical temperature for the deconfinement transition with increasing magnetic field is obtained for $G_s(eB)$, contrasting with the increasing pseudo-critical temperature for G_s^0. The $G_s(eB)$ dependence induces a reduction of the Polyakov loop value in the transition temperature region (also seen in LQCD results [4]).

4. Results (finite chemical potential)

Now, by introducing a finite chemical potential, we analyze the impact of the $G_s(eB)$ on the entire phase diagram. The results are displayed in Figs. 2, 3, and 4, where the respective quantities are presented for two magnetic field intensities (0.2 GeV^2 and 0.6 GeV^2) within both models. From Fig. 2, we see that the (partial) chiral restoration is accomplished via an analytic transition (crossover) at low chemical potentials, and through a first-order phase transition at higher chemical potentials. The region on which the chiral phase is broken (black/blue region) shrinks as the magnetic field increases for the $G_s(eB)$ model, and the opposite occurs for G_s^0. Similar plots are shown in Fig. 3, but now for the strange quark. The general

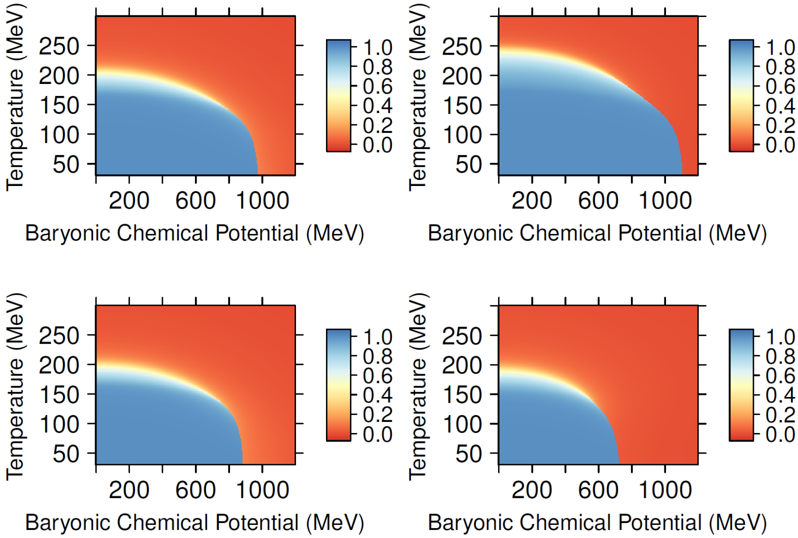

Fig. 2. (Color online) Up-quark condensate (normalized by its vacuum value) with G_s^0 (top) and $G_s(eB)$ (bottom) for $eB = 0.2$ GeV^2 (left) and $eB = 0.6$ GeV^2 (right). The color scale represents the magnitude of the vacuum normalized condensate.

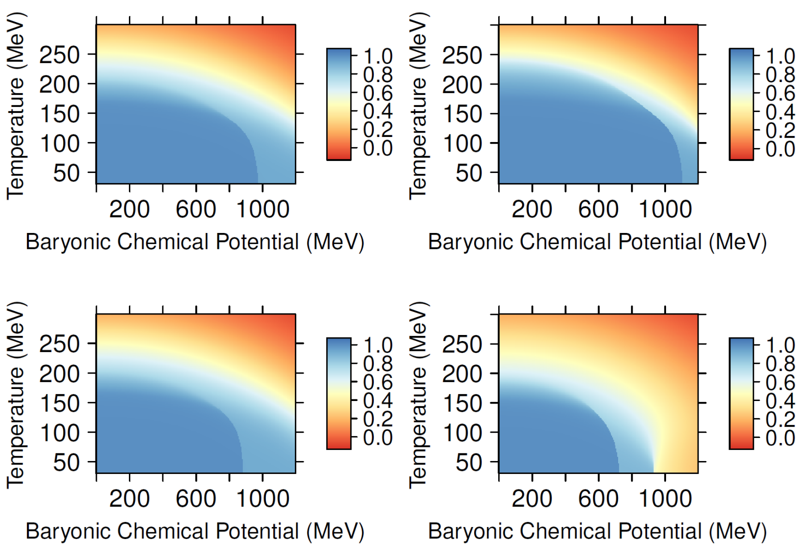

Fig. 3. Strange-quark condensate (normalized by its vacuum value) with G_s^0 (top) and $G_s(eB)$ (bottom) for $eB = 0.2$ GeV^2 (left) and $eB = 0.6$ GeV^2 (right). The color scale represents the magnitude of the vacuum normalized condensate.

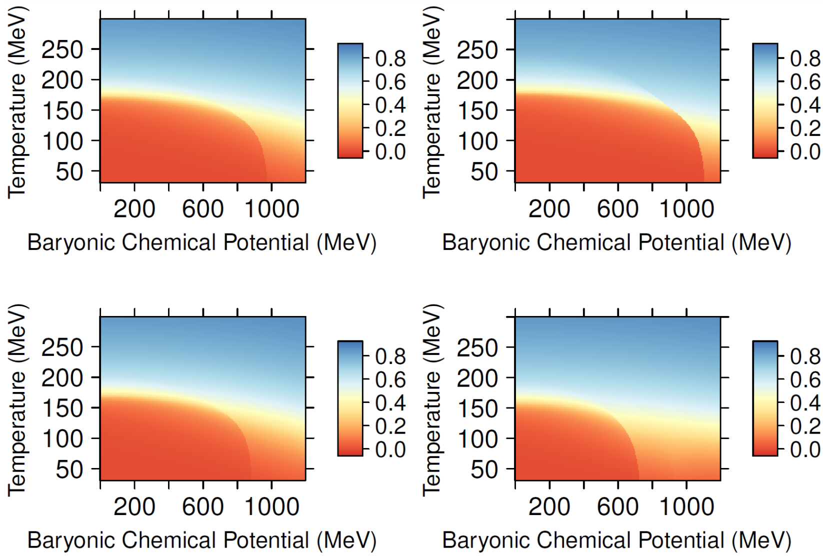

Fig. 4. Polyakov loop value Φ with G_s^0 (top) and $G_s(eB)$ (bottom) for $eB = 0.2$ GeV^2 (left) and $eB = 0.6$ GeV^2 (right). The color scale represents the Polyakov loop magnitude.

pattern shows a smoothly decrease of the strange quark condensate over the whole phase diagram, though some discontinuities appear, which are induced by the first-order phase transition of the light quarks. An interesting result is seen for the $G_s(eB)$ model at $eB = 0.6$ GeV^2 (bottom right panel of Fig. 3): a first-order phase transition shows up for the strange quark at low temperatures which ends up in a Critical End Point (CEP) at a temperature around 50 MeV. Finally, we represent the Polyakov value in Fig. 4. The general pattern is maintained within both models. We see that the transition from confined quark matter ($\Phi \approx 0$) to deconfinement quark matter ($\Phi \approx 1$) is accomplished via an analytic transition, reflected in the continuous increase of the Polyakov loop value (there is a discontinuity induced by the chiral first-order phase transition on which the variation of the Polyakov loop value is small). Because the chiral broken phase region gets smaller with an increasing magnetic field, the region on which the chiral phase is (approximately) restored but still confined (at low temperatures and high chemical potentials) enlarges with an increasing magnetic field strength. The opposite occurs for the model with a constant coupling.

As a final step, we focus on the CEP's location of the chiral transition as a function of the magnetic field [9, 10]. The result is shown in Fig. 5. An important result shows up that clearly differentiates both models. Despite the agreement at low magnetic field strengths ($eB < 0.1$ GeV^2) between both models on how the CEP reacts to the B presence, for higher magnetic fields the CEP moves towards lower chemical potentials for $G_s(eB)$, while it moves for higher chemical potentials for G_s^0. This might indicate that for high enough magnetic fields, the chiral transition might change from an analytic to a first-order phase transition at zero chemical potential when the IMC effect is considered (there are some indications for this scenario [11]).

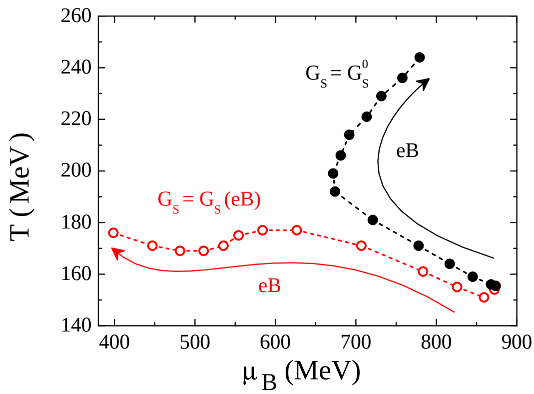

Fig. 5. (Color online) The CEP position with increasing B field for G_s^0 (black) and $G_s(eB)$ (gray/red).

This work was partly supported by the Project PEst-OE/FIS/UI0405/2014 developed under the initiative QREN financed by the UE/FEDER through the program COMPETE — "Programa Operacional Factores de Competitividade", and by grants Nos. SFRH/BD/51717/2011 and SFRH/BPD/102273/2014 from F.C.T., Portugal.

REFERENCES

[1] V.A. Miransky, I.A. Shovkovy, *Phys. Rep.* **576**, 1 (2015).
[2] G.S. Bali *et al.*, *J. High Energy Phys.* **1202**, 044 (2012).
[3] G.S. Bali *et al.*, *Phys. Rev. D* **86**, 071502 (2012).
[4] F. Bruckmann, G. Endrődi, T.G. Kovács, *J. High Energy Phys.* **1304**, 112 (2013).
[5] J.O. Andersen, W.R. Naylor, A. Tranberg, *Rev. Mod. Phys.* **88**, 025001 (2016).
[6] S. Roessner, C. Ratti, W. Weise, *Phys. Rev. D* **75**, 034007 (2007).
[7] P. Rehberg, S.P. Klevansky, J. Hufner, *Phys. Rev. C* **53**, 410 (1996).
[8] M. Ferreira *et al.*, *Phys. Rev. D* **89**, 116011 (2014).
[9] P. Costa *et al.*, *Phys. Rev. D* **89**, 056013 (2014).
[10] P. Costa *et al.*, *Phys. Rev. D* **92**, 036012 (2015).
[11] G. Endrődi, *J. High Energy Phys.* **1507**, 173 (2015).